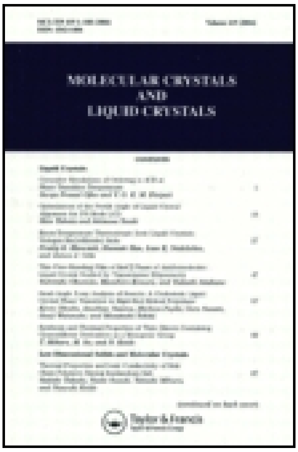

Molecular Crystals and Liquid Crystals
Publication details, including instructions for authors and subscription information:
http://www.tandfonline.com/loi/gmcl20

The Optical and Electrical Characterization of Solar Cell Devices Based on the Physical Parameters of P3HT:PCBM Photoactive Layers

Yoonseog Song [a] & Sang Ouk Ryu [a]
[a] Department of electronics engineering, Dankook University, San #29, Anseo-dong, Cheonan-si, Chungcheongnam-do, 330-714, South Korea

Version of record first published: 30 Aug 2012.

To cite this article: Yoonseog Song & Sang Ouk Ryu (2012): The Optical and Electrical Characterization of Solar Cell Devices Based on the Physical Parameters of P3HT:PCBM Photoactive Layers, Molecular Crystals and Liquid Crystals, 565:1, 22-31

To link to this article: http://dx.doi.org/10.1080/15421406.2012.691001

Mol. Cryst. Liq. Cryst., Vol. 565: pp. 22–31, 2012
Copyright © Taylor & Francis Group, LLC
ISSN: 1542-1406 print/1563-5287 online
DOI: 10.1080/15421406.2012.691001

The Optical and Electrical Characterization of Solar Cell Devices Based on the Physical Parameters of P3HT:PCBM Photoactive Layers

YOONSEOG SONG AND SANG OUK RYU*

Department of electronics engineering, Dankook University, San #29,
Anseo-dong, Cheonan-si, Chungcheongnam-do 330-714, South Korea

In this study, we investigated the power conversion efficiency of organic solar cells utilizing conjugated polymer/fullerene bulk-hetero junction device structures. We fabricated Poly(3-hexylthiophene)(P3HT) as an electron donor, [6,6]-Phenyl C_{61} *butyric acid methyl ester(PCBM) as an electron acceptor, and Poly(3,4-ethylenedioxythiophene) - poly(styrenesulfonate(PEDOT:PSS)as a hole injection layer(HIL). These materials were coated using a spin coating method onto a glass substrate. The properties of the fabricated organic solar cell (OSC) devices have been analyzed as a function of the mixture ratios ranging from 1:0.4 to 1:1.3 (the P3HT was fixed at 1). The electrical characteristics of the fabricated devices were obtained by investigating the J-V, the fill factor (FF), and power conversion efficiency (PCE). The highest PCE (2.2%) was obtained after a post annealing at 150°C at the mixture ratio of 1:0.7, which is 2.2times better than the device without post-annealing.*

Keywords Solar cell; P3HT; PCBM; annealing; conjugated polymers; fullerenes; bulk hetero; junction; PCE

Introduction

In the last few years, an increased effort has been put into the development of solar cells based on organic molecules and conjugated polymers [1–6]. However, the low efficiency of these OSCs, when compared to silicon based solar cells, limits their feasibility for commercial use [7]. The efficiency of OSC devices is mainly limited by several factors. For example, the high energy band gap of the materials used also limits the capability to harvest the photo generated charges at lower sunlight energies. More importantly, the charge carrier mobility of the organic materials is very low. The poor organic thin film conductivity significantly cuts down on the output power conversion efficiency [8,9]. Major progress in the power conversion efficiency has been achieved by introducing the bulk hetero junction (BHJ) concept that replaces the bi-layer structure [10,11]. Therefore, huge efforts have already been taken in order to improve their photovoltaic performance. The BHJ structure provides not only high surface contacts for the charge separation, but also an interpenetrating network that enables an efficient charge transport [12]. The essential parameters of the PV cells which determine the power conversion efficiency (PCE) are the open circuit

---

*Address correspondence to Prof. Sang Ouk Ryu, Department of Electronics Engineering, Dankook University, Anseo-dong, Cheoan 330-714, Korea (ROK). Tel.: (+82)41-550-3576; Fax: (+82)41-550-3041. E-mail: ryuso@dankook.ac.kr

voltage (V_{oc}, V), the short circuit current density (J_{sc}, mA/cm^2), and the fill factor (FF,%). Recently, many groups have expended great effort in order to enhance these parameters. For example, tandem or stacking structures have been proposed in order to enhance the efficiency. Narrow band gap polymer materials have been adopted for use as an active material [13–15].

Among those factors, the P3HT:PCBM mixture ratio is another important factor that needs to be considered [17]. The effect of the annealing process on the organic solar cells, especially in the view of the nanoscale morphology has also been reported by H. Hopper et al. [18].

In this study, we have characterized the electrical performances of OSCs based on a BHJ structure. We analyzed the electrical characteristics based on three physical parameters: the mixture ratio of the P3HT:PCBM, the active layer thickness, and the annealing temperature used for the devices. We used the hetero junction structure of poly(3-hexylthiophene)(P3HT) and [6, 6]-phenyl C_{61}-butyric acid methyl ester (PCBM-C_{61}, 99%). The P3HT, an electron donor, was obtained from Rieke Metals (absorption wavelength 443–568 nm); the PCBM, an electron acceptor, was obtained from NANO-C (absorption wavelength 284–341nm).

Experimental

The fabricated OSCs in this study consist of a photoactive layer consisting of P3HT:PCBM-C_{61}, based on the BHJ structure. The photoactive materials, the P3HT and the PCBM-C_{61}, were prepared by dissolving them in O-Dichlorobenzene(1,2-Dichlorobenzene)(1.2wt%) and then stirred for 12 hours in order to ensure complete dissolution. The P3HT and PCBM solutions were mixed at the ratios of 1:0.4, 1:0.7, 1:1, and 1:1.3 by weight.

The ITO coated soda lime glass was cleaned with acetone, methanol, and de-ionized water in an ultrasonic bath in order to remove any contaminants on the substrates. Iso-propyl alcohol (IPA) was used to remove the water pollutants. The prepared ITO substrates were patterned using a contact aligner and etched with acid ($HCl:HNO_3:H_2O$). The cleaned ITO substrates were then treated by a plasma surface treatment with an $O_2/Ar = 2/1$ mixtures for 90 seconds. The treatment used a power of 150W RF in order to improve the interface conditions between the organic material and the ITO and also to remove the native-oxide film on ITO substrate. The polyethylenedioxythiopene:poly-styrenesulfonate(PEDOT:PSS), used as a hole injection layer (HIL), was deposited using a spin coating method on the ITO substrate and baked at 90°C for 1 hour to dry the solvents. We fabricated three different thicknesses for the active layers ranged from 30nm to 100 nm. After the photoactive layer was coated, pristine Al(150nm) metal electrodes were subsequently deposited on the active layer by means of a metal evaporator(SUNICELL PLUS 200) under the high vacuum conditions of 5×10^{-8} torr. All of the fabricated devices were post-annealed in a vacuum oven at 150°C for 10 min. All of the solution stirring and spin coating processes were conducted under ambient conditions. The fabricated devices were classified by their photoactive layer thicknesses, mixture ratios, and post-annealing temperatures.

All of the light absorption layers had the same 4×4 mm^2 dimensions. The fabricated solar cell structures and the energy band diagrams are shown in Figs. 1 (a) and (b). The thicknesses of each active layer were measured utilizing a spectroscopic ellipsometer (VB-400). The optical absorption spectrums were investigated using UV-vis spectroscopy (UV 1601PC UV-visible Photometer). The power conversion efficiencies (PCE) were calculated from the current density-voltage (J-V) characteristics and the fill factor (FF) under

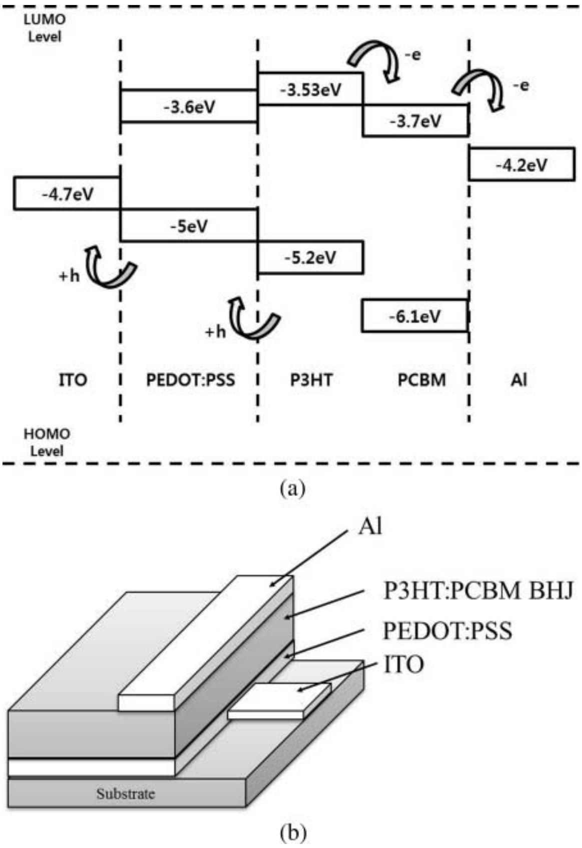

Figure 1. (a) An energy band gap diagram of the fabricated organic solar cell, (b) the cross sectional view of the fabricated devices used in this study.

a simulated solar light irradiation of 100 mW/cm^2 under the ambient conditions (an ORIEL solar simulator with 150W Xe lamp and a KEITHLY SMU 2400). Before the devices were measured, the light source was calibrated using a reference cell (ORIEL Solar reference cell).

Results and Discussion

The chemical structures of the materials used in this study are shown in Fig. 2. These materials are known to have good absorption characteristics in the visible range (P3HT $\approx$560 nm, PCBM-C$_{61}$ $\approx$335 nm). By the utilization of the active layers, the BHJ device structure has been studied. The structure of the devices and the energy band diagrams of each layer are depicted in Fig. 1. In order to overcome one of the main limitation factors, i.e. the charge separation problem in organic photovoltaic devices the BHJ structure was used. After evaporating the Al contact layer, the fabricated devices were annealed at 150°C for 10 min. The effect of the post-annealing process has been reported by H. Hoppe et al. and Chirvase *et al*. [18,19]. According to the report, the performance of the photoactive layer was degraded at high temperatures caused by a large PCBM aggregation. Therefore the photovoltaic characteristics dependence on the annealing temperature is an important

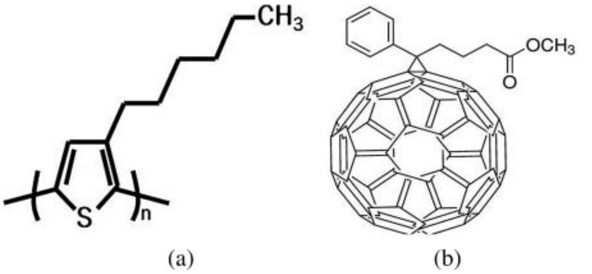

Figure 2. The chemical structures used in the bulk hetero junction active layer: (a) P3HT, (b) PCBM-C_{61}.

factor in the improvement of device performance. The P3HT:PCBM mixture ratio is another factor which influences device performance. According to Chen *et al*, the P3HT:PCBM active layer has shown a broad range of optical properties based on its mixing ratio [21]. In this study, the mixing ratio has been finely tuned to have more optimized results.

The current density-voltage (J-V) characteristics were analyzed utilizing a KEITHLY SMU 2400. The devices were exposed under an AM 1.5 illumination with a calibrated solar simulator (ORIEL reference cell) having an intensity of 100mW/cm^2. The electrical characteristics of the investigated devices are shown in Fig. 3. Figure 3 (a) shows the current density-voltage characteristics of the as-deposited active layer. As seen in the figure the best results were obtained at the mixture ratio of 1:0.7 (P3HT:PCBM). However, as shown in Fig. 3 (b), these results were dramatically improved after the post-annealing process. As summarized in Table 1, the overall performance based on the mixture ratio kept the same order before and after the annealing process. However, the PCE of the mixture ratio of 1:0.7 showed more than a two-fold improvement. The results showed not only an increase in the J_{sc} and Voc but also a great increase in the shunt resistance (2.21 to 4.28 kΩ) and a decrease in the series resistance (0.159 to 0.095 kΩ). In order to find out the optimum annealing conditions the active layers were annealed at different temperatures. Figure 4 shows the current density-voltage (J-V) characteristics under the different annealing conditions. The PCEs increased until 150°C from 0.9% to 2.2% in accordance with the J_{sc} (from 6.6 to 7.6 mA/cm^2) and the V_{oc} (from 0.383 to 0.505 V). According to H. Hoppe et al, their annealing experiments resulted in micrometer sized PCBMs [18]. Although the size of the organic PCBM is important, the interfacial properties are another important factor to improve the PCE in the device characteristics. As summarized in Table 2, J_{sc} and Voc showed little increase according to the annealing temperature whereas the shunt resistance (R_{shunt}) and the series resistance (R_{series}) showed a much larger change, which implies that at a 150°C annealing temperature, the interface between the active layer and the electrode obtains its most stable conditions. Further annealing resulted in a deterioration of the device performance, which might originate from the morphological degradation due to excessively large PCBM domains, as mentioned by Hoppe [18]. Therefore, the morphological stability and also the device interfacial properties in organic solar cells are issues to be addressed.

Figure 5 shows the absorption spectra of solar cells having a different mixture ratio of P3HT:PCBM. According to the results of Fig. 3, we expected that a 1:0.7 mixture ratio would exhibit the highest absorption intensity. However the highest absorption intensity was found at a mixture ratio of 1:0.4. Obviously, the intensity of the UV-vis absorption peaks increased with the P3HT molecules. Furthermore, when the P3HT:PCBM ratio was 1:0.7, we could clearly observe the three vibronic shoulders, indicating strong interchain interlayer

Table 1. The electrical characteristics of each devices classified according to the P3HT:PCBM mixture ratio and the annealing condition

	P3HT:PCBM							
	As-deposited				Post Annealed at 150°C			
Materials	1:0.4	1:0.7	1:1	1:1.3	1:0.4	**1:0.7**	1:1	1:1.3
PCE (%)	0.566	1	0.870	0.684	1.3	**2.2**	1.6	0.929
F.F (%)	41.3	47.1	50.8	45	46.6	**56.5**	50.7	30.3
J_{sc} (mA/cm^2)	3.8	5.2	4.3	3.2	6	**7.6**	6.6	5.8
V_{oc} (V)	0.363	0.414	0.394	0.474	0.464	**0.505**	0.484	0.525
R_{shunt}.(kΩ)	1.54	2.21	2.91	3.2	1.82	**4.28**	3.77	0.999
R_{series}.(kΩ)	0.202	0.159	0.146	0.329	0.147	**0.095**	0.144	0.419

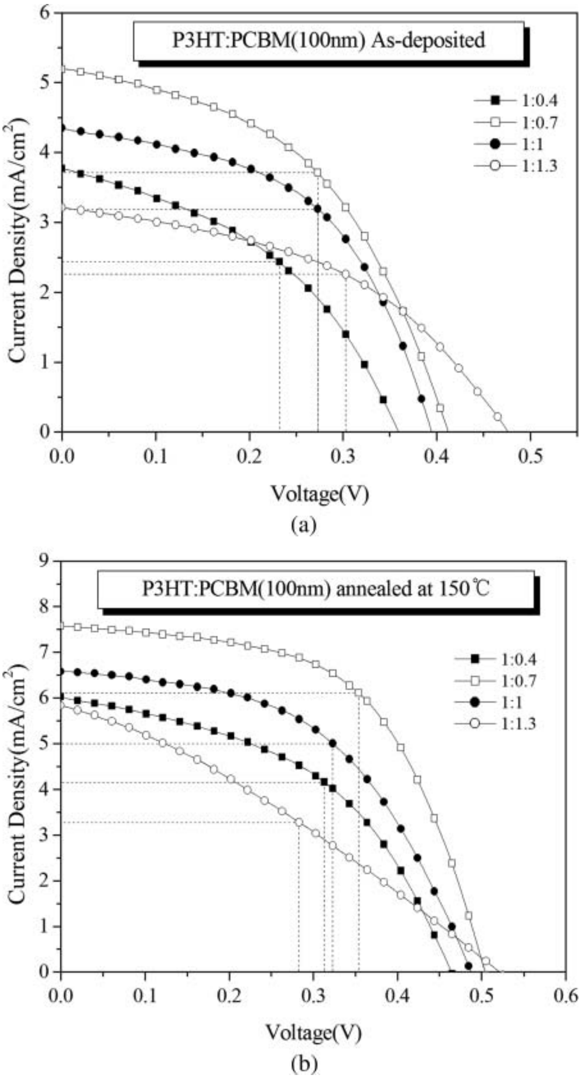

(a)

(b)

Figure 3. The current density-Voltage (J-V) characteristics of: (a) P3HT:PCBM(100 nm) as-deposited, (b) P3HT:PCBM(100 nm) post annealed at 150°C for the different P3HT:PCBM mixture ratios.

interactions among the regioregular P3HT chains and a high ordering of the polymer chains in the composition films [20]. However, the vibronic peaks gradually disappeared with an increase of the PCBM concentrations, suggesting that the interaction of the P3HT polymer chains was disrupted by the PCBM molecules [21]. The reduced interaction of the P3HT would lower the hole mobility, thereby decreasing the efficiency and the current of the OSCs, especially for the samples in which the PCBM content was over 40%. Despite the higher absorption characteristic of the 1:0.4 mixture ratio, the resulting PCE performance did not match with the optical characteristics, which may stem from the device issues, as mentioned before.

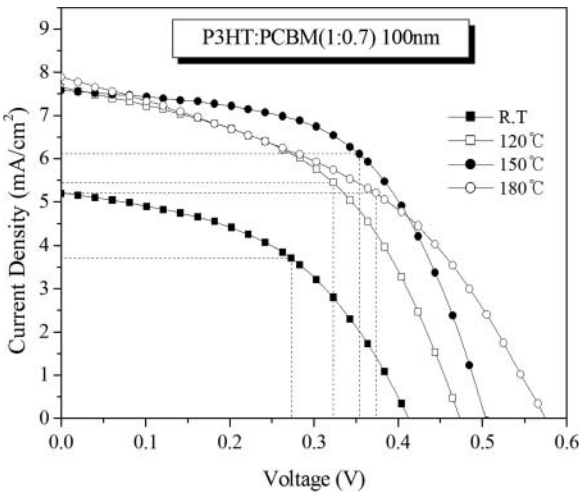

Figure 4. The current density-Voltage (J-V) characteristics of fabricated devices after post annealing at different temperatures (the mixing ratio was fixed at 1:0.7).

Figure 6 shows the J-V characteristics of the P3HT:PCBM (1:0.7) as a function of the photoactive layer thicknesses. The thickness of the active layer was measured by an ellipsometer; the thickest layer was around 100nm. We observed that the thicker active layers tend to show better light absorption characteristics. According to the Lambert-Beer law:

$$\mathbf{T} = \mathbf{I}/\mathbf{I_0} = \mathbf{10}^{-\alpha\ell} \tag{1}$$

where **I** and $\mathbf{I_0}$ are the intensity of the incident light and the transmitted light, respectively. **T** is the transmissivity, $\boldsymbol{\alpha}$ is the absorption coefficient of the substance, and $\boldsymbol{\ell}$ is the distance the light travels through the material. For our determinations we used the same active layer parameters except for the thickness, therefore the transmittance is solely dependent on the parameter $\boldsymbol{\ell}$. A thicker sample, therefore, has a lower transmittance (a higher light absorption), as shown in Fig. 7. Generally, more light absorption leads to photo generated charges. Therefore the electrical characteristics should be improved for a thicker photoactive

Table 2. The electrical characteristics of the P3HT:PCBM (1:0.7) active layer after processing at the different post annealing temperatures

	P3HT:PCBM			
Materials	R.T	120°C	150°C	180°C
PCE (%)	0.9	1.8	**2.2**	1.9
F.F (%)	37	48.5	**56.5**	42.9
J_{sc} (mA/cm^2)	6.6	7.6	**7.6**	7.9
V_{oc} (V)	0.383	0.474	**0.505**	0.575
R_{shunt} (kΩ)	0.699	1.55	**4.28**	1.17
R_{series} (kΩ)	0.171	0.112	**0.095**	0.163

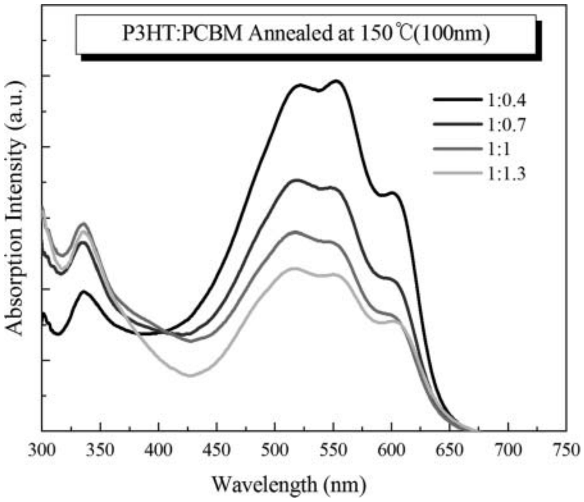

Figure 5. The UV absorption intensity curves of the devices after post annealing at 150°C using different mixture ratios.

layer. In a previous study, M. Lenes *et al*. reported that increasing the photoactive layer thickness does not necessarily result in a higher power conversion efficiency, because the increase in the short circuit current is canceled by a decrease in the fill factor. They also insisted that the decrease in the fill factor originates from the occurrence of a space-charge limited regime in the photocurrent and in recombination losses [16]. Though we could not experiment with a thicker active layer than 100 nm because of the nature of the spin-coating process (it becomes difficult to obtain a high quality thin film surface), we estimate that the thickness has a good valence in the short circuit current and light absorption properties. The best performance was at FF = 56.6%, PCE = 2.2% at the thickness of 100 nm. Compared

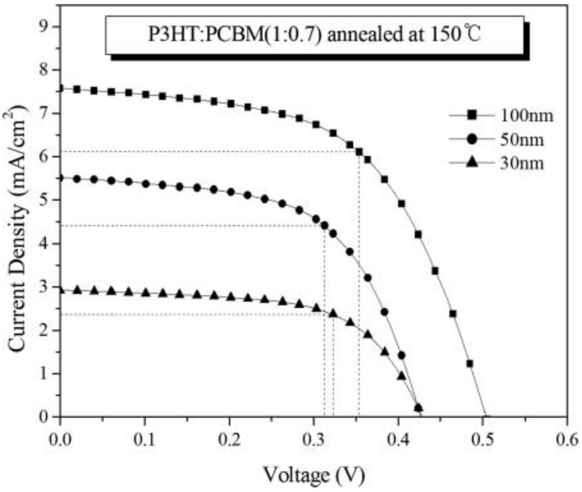

Figure 6. The current density-Voltage (J-V) characteristics of the devices with a 1:0.7 P3HT:PCBM active layer as a function of thickness.

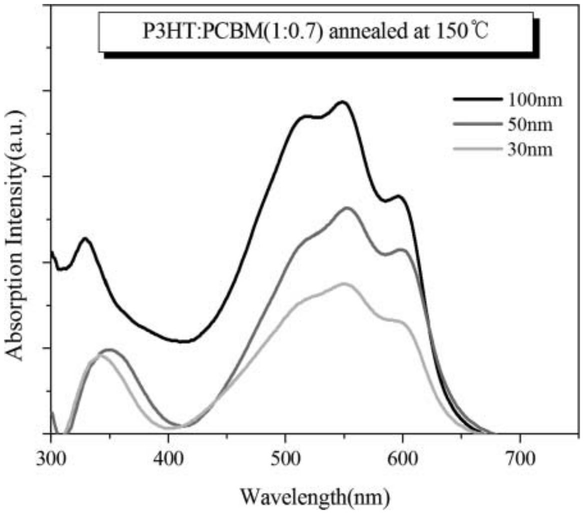

Figure 7. The UV absorption intensity curves of the devices with a 1:0.7 P3HT:PCBM active layer after post annealing at 150°C as a function of thickness.

to the thinner device (30nm), the performances the V_{oc} and the J_{sc} were much improved. As a result, the calculated PCE increased from 0.7% to 2.2%.

Conclusions

We studied solar cells based on a organic P3HT:PCBM bulk hetero junction system. The device performance was mainly dependent on the P3HT:PCBM mixture ratio, the annealing condition of the active layers, and the thickness of the active layer. After the fine tuning of the P3HT:PCBM mixture ratio it was found that the best power conversion efficiency was obtained at the ratio of 1:0.7 (P3HT:PCBM). The best efficiency was shown when it was annealed at 150°C. The resulting data showed a $J_{sc} = 7.6\text{mA/cm}^2$, a $V_{oc} = 0.505\text{V}$, an FF = 56.6% and a PCE = 2.2% at a thickness of 100 nm. The data tends to show a better PCE for a thicker active layer; however, as discussed previously, there is an optimum thickness for the best performance due to the mobility of the electrons or holes before they get recombined. We also observed that the device characteristics were determined not only by the properties of the polymer active layer but also by the interfacial properties between the active layer and the electrode material. We found that in many cases the device performance was influenced by the shunt resistance and the series resistance rather than by the short circuit current and the open circuit voltage.

Acknowledgment

This research was supported by Basic Science Research Program through the National Research Foundation of Korea (NRF) funded by the Ministry of Education, Science and Technology (2011-0006992).

References

[1] Sariciftci, N. S., Smilowitz, L., Heeger, A. J., & Wudl, F. (1992). *Science.*, *258*, 1474.

[2] Brabec, C. J., Padinger, F., & Sariciftci, N. S. (1999). *J. Appl. Phys.*, *85*, 6866.

[3] Morita, S., Zakhidov, A. A., & Yoshino, K. (1992). *Solid State Commun.*, *82*, 249.

[4] Brabec, C. J., Padinger, F., Hummelen, J. C., Janssen, R. A. J., & Sariciftci, N. S. (1999). *Synth. Met.*, *102*, 861.

[5] Brabec, C. J., & Sariciftci, N. S. (1999). in *Semiconducting Polymers* Ed.; Hadziioannou G. and van Hutten P. F.: Wiley-VCH Weinheim.

[6] Granström, M., Petritsch, K., Arias, A. C., Lux, A., Andersson, M. R., & Friend, R. H. (1998). *Nature.*, *395*, 257.

[7] Shaheen, S. E., Brabec, C. J., & Sariciftci, N. S. (2001). *Appl. Phys. Lett.*, *78*, 841.

[8] Blom, P. W. M., De Jong, M. J. M., & Van munster, M. G. (1997). *Phys., Rev.*, *B55*, R656.

[9] Peumans, P., & Forrest, S. R. (2001). *Appl. Phys. Lett.*, *79*, 126.

[10] Tang, C. W. (1986). *Appl. Phys. Lett.*, *48*, 183.

[11] Yu, G., & Heeger, A. J. (1995). *J. Appl. Phys.*, *78*, 4510.

[12] Kraabel, B., Hummelen, J. C., Vacar, D., Moses, D., Sariciftci, N. S., Heeger, A. J., & Wudl, F. (1996). *J. Chem. Phys.*, *104*, 4267.

[13] Li, G., Chu, C. W., Shrotriya, V., Huang, J., & Yang, Y. (2006). *Appl. Phys. Lett.*, *88*, 253503.

[14] Wienk, M. M., Turbine, M. G. R., Struijk, M. P., Fonrodona, M., & Janssen, R. A. J. (2006). *Appl. Phys. Lett.*, *88*, 153511.

[15] Shao, Y., & Yang, Y. (2005). *Adv. Mater. Weinheim.*, *17*, 2841.

[16] Lenes Mand Koster, L. J. A. (2006). *Appl. Phys. Lett.*, *88*, 243502.

[17] Manceau, M., Chambon, S., Rivaton, A., Gardette, J. L., Guillerez, S., & Lemaître, N. (2010). *Sol. Energy. Mater. Sol. Cells.*, *94*, 1572.

[18] Hoppe, H., Niggemann, M., Winder, C., Kraut, J., Hiesgen, E., Hinsch, A., Meissner, D., & Sariciftci, N. S. (2004). *Adv. Funct. Mater.*, *14*, 1005.

[19] Chirvase, D., Parisi, J., Hummelen, J. C., & Dyakonove, V. (2004). *Nanotechnology.*, *15*, 1317.

[20] Li, G., Shrotriya, V., Huang, J. S., Yao, Y., Moriarty, T., Emery, K., & Yang, Y. (2005). *Nat. Mater.*, *4*, 864.

[21] Chen, F. C., Ko, C. J., Wu, J. L., & Chen, W. C. (2010). *Sol. Energy. Mater. Sol. Cells.*, *94*, 2426.